

WIDEBAND PLANAR SPLIT RING RESONATOR BASED METAMATERIALS

Abdolshakoor Rigi-Tamandani*, Javad Ahmadi-Shokouh, and Saeed Tavakoli

Faculty of Electrical and Computer Engineering, University of Sistan and Baluchestan, Zahedan, Iran

Abstract—In this paper, a method for increasing bandwidth of metamaterial structures is presented. The metamaterial structures used in this study are based on Split Ring Resonators (SRRs), the most recognized structures for realization of metamaterials with negative magnetic permeability coefficients. To increase the frequency bandwidth of such metamaterials, two different methods, 1) rotating the inner ring of SRR with different angles in a hybrid structure, which is herein called unit cell, 2) changing dimensions of SRR, are presented. Moreover, the effect of SRR arrangement in unit cell on bandwidth is investigated. The idea of bandwidth enhancement is verified via simulations, which are performed via full-wave method and measurements, which are done using a built strip-line setup.

1. INTRODUCTION

Metamaterials are artificial materials that show negative permittivity and/or negative permeability over a limited frequency bandwidth [1–3]. Since the negative permittivity naturally occurs in metals, as described by the Drude electron model in metals [4], Epsilon-negative (ENG) materials are easy to realize. However, the acquisition of the Mu-negative (MNG) is a real challenge since there are no free magnetic charges in nature [1, 2]. Artificially built metamaterials with negative permeability are suitable alternative though. Resonator structures such as Split-Ring Resonators (SRRs) [2], S-shaped resonators [5], Ω -shaped resonators [6], Spiral Resonators (SRs) [7] are classified in this group, and have negative permeability in certain frequency ranges.

Received 3 December 2012, Accepted 9 January 2013, Scheduled 17 January 2013

* Corresponding author: Abdolshakoor Rigi-Tamandani (a.r.tamandani@gmail.com).

One of major obstacles for the practical applications of these MNG materials lies in the bandwidth limitation where the bandwidth they demonstrate is quite narrow. Some efforts have been devoted to overcoming this weakness [8–12]. In some of these researches, increasing bandwidth has been studied only via mathematical models [8, 9]. To the best of the authors' knowledge, two methods have been proposed in the literature in order to increase the bandwidth. One method, introduced by Rudolph and Grbic [13], includes a periodic cage of backward-wave transmission lines. However, it was a three-dimensional structure and hard to fabricate using planar technologies, such as Printed Circuit Boards (PCB) techniques. The other method by Lepetit et al. [14] proposes a construction of all-dielectric MNG with an array of high dielectric-constant photonic crystals. In this method, not only the photonic crystal loss is too high, but also the fabrication process is difficult and costly.

In this paper, we study a composite MNG structure based on SRRs to increase the bandwidth. Interestingly, without resorting to high dielectric constant cylinders or a three-dimensional transmission-line cage, the planar composite SRR structure is quite compatible with standard Printed-Circuit-Board (PCB) fabrication techniques. Hence, it 1) dramatically reduces the complexity of manufacturing process; 2) reasonably accomplishes the mechanical stability of the MNG material's structure. The results show that the proposed structure significantly increases the frequency bandwidth. Moreover, in this paper we study the impact of the SRR's different arrangements on increasing the overall achieved bandwidth. The proposed MNG structure is designed for the low frequency bands specially Very High Frequency (VHF) band as it is recently of interest in antenna miniaturization applications for the Fourth Generation (4G) networks like Long Term Evolution (LTE) 700. Although the proposed scheme in this paper is designed for a certain frequency range, it can be surely used for other frequency bands usually employed in the MNG structures. Moreover, the introduced design as a broadband MNG metamaterial can be used as a periodic unit cell structure, in practice.

The rest of the paper is organized as follows. The problem is stated in Section 2. Section 3 provides the MNG design with SRR. The MNG design with improved bandwidth will be introduced in Section 4. The magnetic permeability coefficient results are presented in Section 5. Section 6 shows the arrangement of SRR in the unit cell and the effect of substrate dielectric loss tangent. In Section 7, the measurement campaign is described. Finally, conclusions are given in Section 8.

2. PROBLEM STATEMENT

For the design and analysis of the metamaterials, two methods have been proposed [15, pages 61–82]: The first technique is based on analytical methods such as the Lorentz theory and circuit models of metamaterials, and the second method is based on full-wave simulations such as Finite Element Method (FEM) and Finite Integration Technique (FIT). The first method can be used only for a limited number of metamaterial structures, and often cannot accurately predict the macroscopic behaviour of the metamaterial. In this paper, we will perform the design and analysis of the proposed metamaterial structures based on the second technique. In this research, the design and analysis procedures are done through the HFSS software.

The MNG design with improved bandwidth is done in two stages. In the first step, three SRRs are designed with different resonant frequencies. Then, the proposed MNG unit cell with a combination of three different SRRs is presented. The idea of multi-resonator structures is to use several different SRRs in a unit cell. These SRRs are designed to have different resonant frequencies. These frequencies can be adjusted very close to each other to provide wide-band MNG materials. Two practical techniques, as described in the next section, are employed to design the SRRs with different resonant frequencies. Moreover, various SRRs arrangements in the proposed MNG are investigated in order to optimally improve the overall bandwidth.

3. DESIGN OF METAMATERIAL STRUCTURES WITH THREE RESONANT FREQUENCIES

In this section, to design of metamaterial structures with different resonant frequencies, we used two methods, 1) rotating inner ring, and 2) changing dimensions of SRR, as follows.

3.1. Rotating Inner Ring of SRR

We can change resonant frequency by rotating the inner ring of SRR [16]. As stated before, our design is performed in the low frequencies which are useful for LTE 700 applications. Hence, we produce three nearly shifted resonant frequencies: 600 MHz, 666 MHz and 775 MHz. To do so, we design three different inner ring rotated SRRs which operate in three nearby different resonant frequencies. The base SRR structure, which we use in this research, is presented in Fig. 1. All the designed metamaterials are performed on a FR4

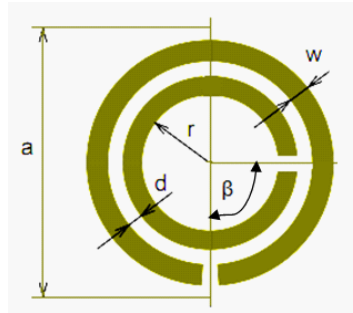


Figure 1. Unit cell configuration.

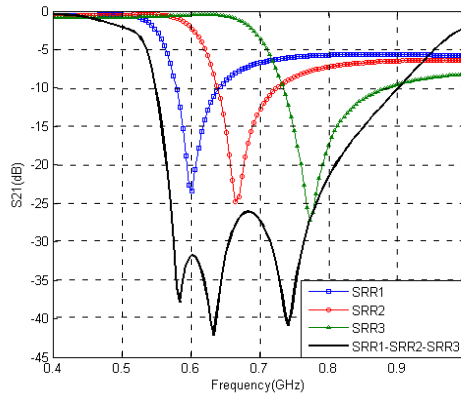


Figure 2. Transmission responses of proposed SRR structures with rotated inner rings.

substrate with a thickness of 2.4 mm. The first metamaterial, herein called SRR1, is constructed with the following dimensions designed in the 600 MHz frequency.

$$r = 9.5 \text{ mm}, \quad w = 0.5 \text{ mm}, \quad d = 0.5 \text{ mm}, \quad a = 25 \text{ mm},$$

$$\beta = 47^\circ \text{ (angle between the two splits)}$$

The next step is to design the second MNG structure, which in this paper is called SRR2, with the same dimensions of SRR1 but $\beta = 33^\circ$. For this design the resonant frequency is 666 MHz. The third structure, called SRR3, with the same dimensions of SRR1 but $\beta = 10^\circ$ has a resonant frequency of 775 MHz. Transmission responses of all these structures are shown in Fig. 2.

As seen in Fig. 2, all three of these structures have the same

bandwidth but shifted in frequency. Hence, it appears that using a suitable combination of these three SRRs one can achieve a broadband MNG metamaterial structure. In the next section, such a structure is presented.

3.2. Changing SRR Dimensions

In this procedure, we take the SRR structure presented in Fig. 1 as the MNG metamaterial. Hence, the first MNG structure herein used, called SRR1, is made on a FR4 substrate of 2.4 mm thickness with the following dimensions which provide a design with 500 MHz resonant frequency.

$$r = 7.5 \text{ mm}, w = 0.5 \text{ mm}, d = 0.2 \text{ mm}, a = 20 \text{ mm}$$

Then, we design another MNG structure with the same SRR1, called SRR2, with the below-mentioned dimensions. This design has a resonant frequency of 600 MHz.

$$r = 7.6 \text{ mm}, w = 0.5 \text{ mm}, d = 0.4 \text{ mm}$$

The third structure, called SRR3, is the next design which has a resonant frequency at 700 MHz with the following dimensions.

$$r = 7 \text{ mm}, w = 0.6 \text{ mm}, d = 0.6 \text{ mm}$$

Transmission responses of these designed structures are shown in Fig. 3.

As seen in Fig. 3, all three of these structures have the same bandwidth but shifted in frequency. Thus, this technique, i.e., a

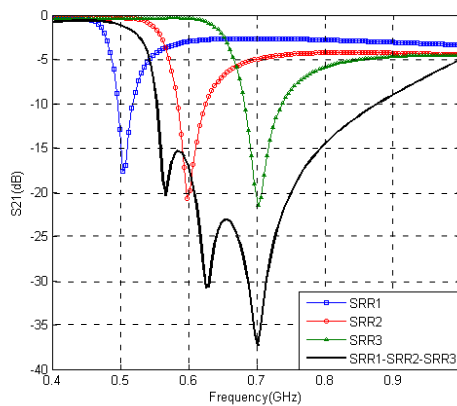


Figure 3. Transmission response of the proposed SRR structures with re-dimensioned SRRs.

suitable combination of three dimensioned SRRs, also appears to provide a broadband MNG metamaterial structure. In this paper, due to simplicity of SRR implementation we take the first method in order to compare the simulation and measurement results.

4. DESIGN OF MNG WITH IMPROVED BANDWIDTH

Based on the results drawn from the previous section, when three SRRs are used in the unit cell, three different resonant frequencies are observed for the total permeability. These resonant frequencies can be adjusted either far from each other, to provide multi-band MNG material, or close to each other to propose a wide-band MNG material. This idea is similar to the combined narrow band filters method to develop a filter with wider bandwidth [17].

In this section, three SRR structures, designed based on the rotating inner ring approach described in the previous section, are combined in a single cell in order to increase bandwidth, as shown in Fig. 4.

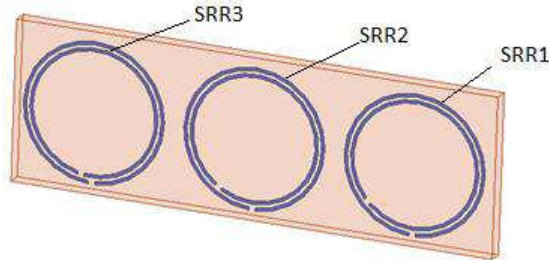


Figure 4. Unit cell structure composed of three SRR with different angles.

The transmission response of the proposed structures is shown in Figs. 2 and 3. The transmission response results shown in these figures clearly show a higher bandwidth than MNG structure made of a single SRR.

5. RESULT OF PERMEABILITY

In this section, using the design and simulation results of the previous section, magnetic permeability coefficients are calculated using Chen

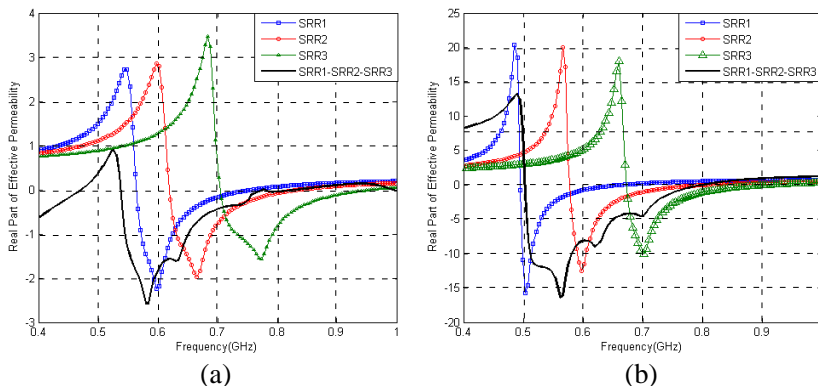


Figure 5. Real part of negative Permeability coefficient for a unit cell with one SRR and a unit cell with three different SRRs. (a) Rotating inner ring. (b) Changing dimensions of SRR.

et al’s algorithm [18] as follows.

$$z = \pm \sqrt{\frac{(1 + S_{11})^2 - S_{21}^2}{(1 - S_{11}) - S_{21}^2}} \quad \text{Re}(z) \geq 0 \quad (1)$$

$$n = \frac{1}{k_0 d} \left\{ \left[\text{Im} \left[\text{Ln} \left(e^{jnk_0 d} \right) \right] + 2m\pi \right] - j \left[\text{Re} \left[\text{Ln} \left(e^{jnk_0 d} \right) \right] \right] \right\} \quad (2)$$

where

$$e^{jnk_0 d} = \frac{S_{21}}{1 - S_{11} \frac{z-1}{z+1}} \quad \text{Im}(n) \geq 0 \quad (3)$$

Moreover, in the above equations k_0 and d are, respectively, the wave number and metamaterial structure thickness. Permeability (μ) of the medium is then computed as:

$$\mu = nz$$

According to Fig. 5, it can be seen that the proposed MNG structure, with a unit cell including three different rings, illustrates a remarkable wide frequency bandwidth compared with the single ring.

6. ARRANGEMENT OF METAMATERIALS IN THE UNIT CELL AND EFFECT OF THE DIELECTRIC LOSS TANGENT

It is shown that the maximum bandwidth achieved by the SRR arrangement in a unit cell should be based on an ascending and/or

descending of resonant frequencies. In other words, the arrangement of SRR in the unit cell shown in Fig. 4 must take one of the following two options of Fig. 6.

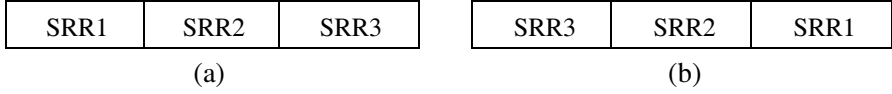


Figure 6. Arrangement of SRR in the unit cell: (a) Ascending, (b) descending.

The same scattering parameters S_{21} and S_{12} show that there is no difference between the above two options, i.e., the ascending/descending resonant frequency arrangements. To verify this achievement, we test two other layouts[†] as Fig. 7.



Figure 7. Two different arrangement of SRR in the unit cell.

For all aforementioned arrangements, including a proposed resonant frequency ascending layout, the transmission responses (S_{21}) are shown in Fig. 8.

As shown in Fig. 8, the proposed arrangement, i.e., ascending/descending, introduces a larger frequency bandwidth than two other structures. Moreover, we study the impact of SRR arrangement on the permeability magnetic coefficient as presented in Fig. 9.

In the aforementioned results, dielectric loss tangent equal to 0.02 is considered for the substrate used in the proposed metamaterials. Now, we consider this loss in our calculations to study how the dielectric loss tangent can affect the bandwidth for the proposed metamaterial. Fig. 10 shows the effect of dielectric loss tangent on the transmission response and negative permeability. The results are plotted for three different loss tangent values. As expected, dielectric loss tangent — like any other loss — reduces the quality factor and frequency selectivity. However, if a substrate with a higher loss tangent is selected, the negative permeability vibrations become smooth (low frequency selectivity and quality factor).

[†] We bring inhere only two configurations among all tested possible combinations. Hence, the achieved results are applied in general.

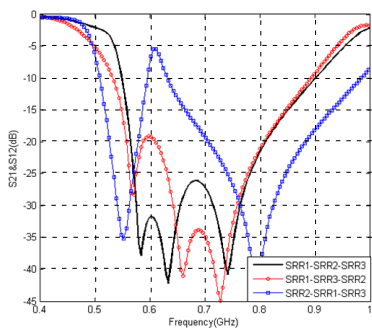


Figure 8. Transmission responses for different SRR arrangements of in the unit cell.

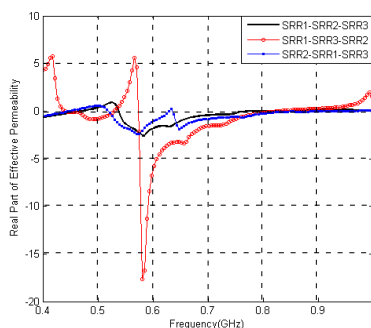
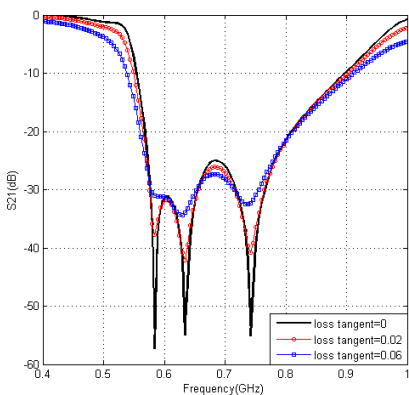
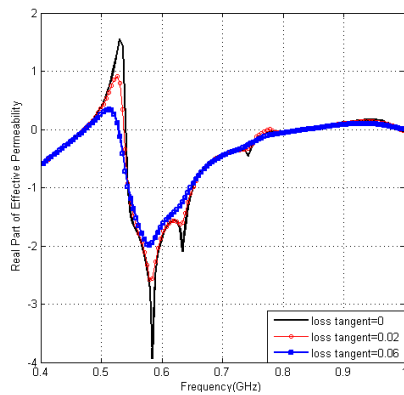


Figure 9. Real part of negative Permeability coefficient for different kind of arrangement of SRR in the unit cell.



(a)



(b)

Figure 10. Effect of the dielectric loss tangent on (a) transmission response, (b) effective permeability.

7. EXPERIMENTAL RESULTS

In order to confirm the validity of our simulation results, empirical campaigns are performed using a strip-line setup which is introduced in [19]. Measurements are performed in two steps: 1) first the unit cell with single ring is measured, 2) then the unit cell with three different rings is measured. In this experiment, all the SRR cells are fabricated using the printed circuit technology on a FR4 substrate material which

has $\varepsilon_r = 4.4$ (see Fig. 11(a)). A three-dimensional metamaterial substrate is then assembled by stacking 45 above-mentioned fabricated strips in the y direction (see Fig. 11(b)). The fabricated metamaterial substrate has dimensions of 10.8 cm, 9 cm, and 5 cm in the y , z , and x directions (see Fig. 11(b)), respectively. The SRR cells are then placed in the middle of a strip-line setup for S -parameter measurements using the methods reported in [19].

The strip-line fixture has dimensions (see Fig. 12(b)) of $l = 27$ cm, $w = 23$ mm (width of strip), $t = 7.5$ cm, $h = 50$ mm (see Fig. 1 in [19]). The fixtures used for characterization of the metamaterial substrate are shown in Fig. 12. The fixture shown in Fig. 12(a) is used to measure the properties of the strip-line without the metamaterial sample. Using

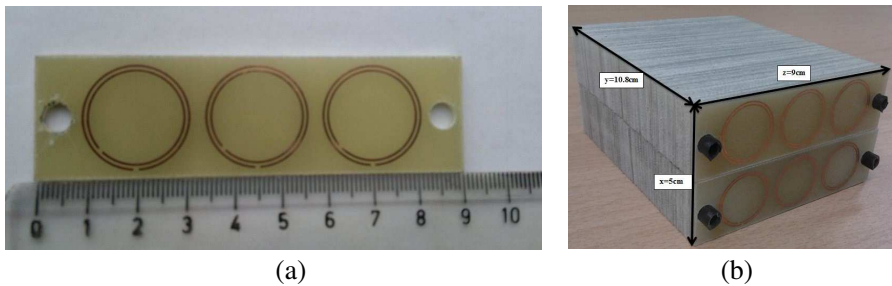


Figure 11. (a) A single strip fabricated using the printed circuit board technology. (b) Fabricated metamaterial substrate.

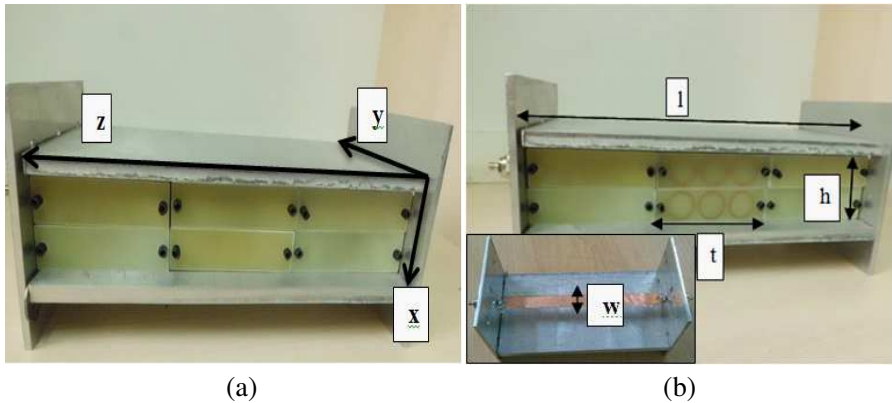


Figure 12. The fabricated strip line fixtures. (a) Without the metamaterial sample (this fixture is used as a reference). (b) With the metamaterial sample to be measured.

this setup, we determine the phase reference plane for the measurement results obtained from the fixture with the metamaterial sample, i.e., Fig. 12(b). Using a vector network analyzer, the S -parameters of the fixture shown in Fig. 12(a) were measured. These parameters are indicated in Figs. 13.

Next, the S -parameters of the fixture with the metamaterial sample as shown in Fig. 12(b) are measured. The magnitude of the measured S -parameters are shown in Fig. 14 and Fig. 15,

Using the measured S -parameters and the analytical method explained in [19], the constitutive parameters of the metamaterial sample are extracted and shown in Fig. 16. The results are then

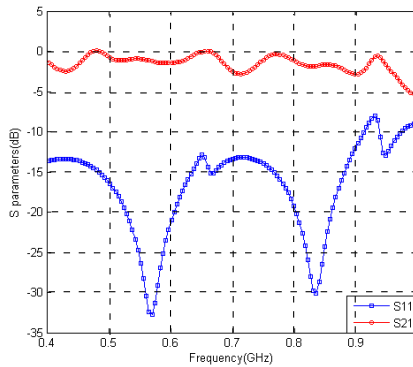


Figure 13. Magnitude of the measured S parameters of the reference fixture (see Fig. 10(a)).

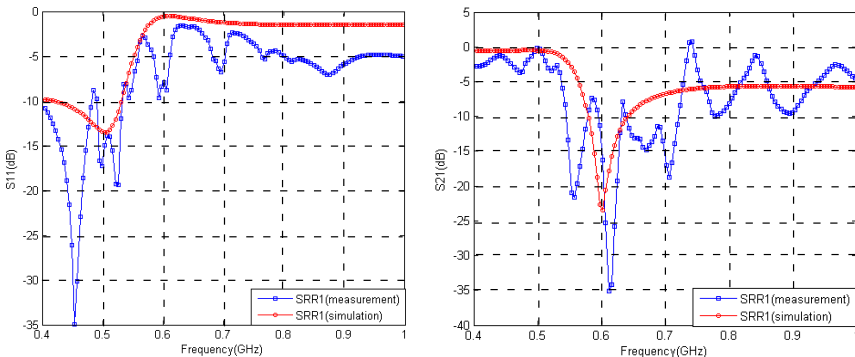


Figure 14. S -parameters of the fixture with the metamaterial sample for unit cell with one SRR.

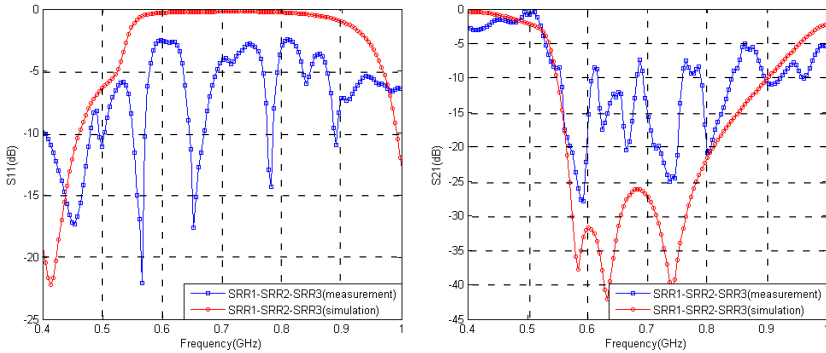


Figure 15. S -parameters of the fixture with the metamaterial sample for unit cell with three different SRRs.

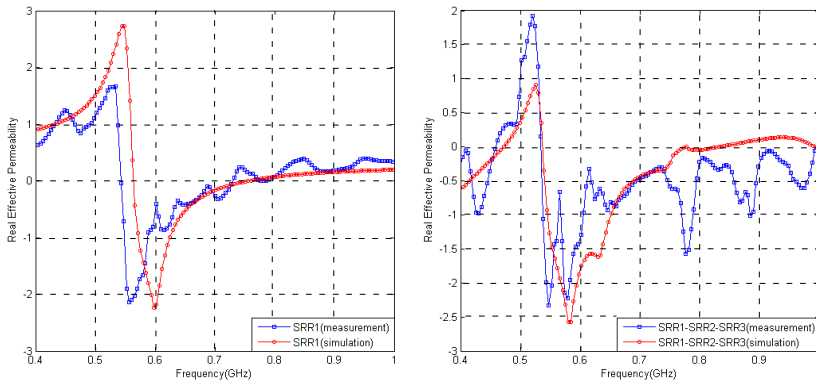


Figure 16. The measured permeability compared with numerical simulation results.

compared with the constitutive parameters extracted numerically from the simulations. As shown in Fig. 16, a good agreement is observed between the simulation and measurement results. It should be noted that in the numerical analysis periodic boundary conditions are used to an infinite number of unit cells. However, in practice we can realize only finite number of unit cells. For example, in the setup used in this work, the fabricated substrate contains 45 unit cells which are stacked in the y direction, and only one unit cell in the x direction. Increasing the number of unit cells provides higher homogeneity in the fabricated substrate, thus it is expected to yield better agreement with measurements.

8. CONCLUSION

In this paper, we propose an effective method to increase the frequency bandwidth of the MNG structures which are constructed based on SRR technique. The proposed structure consists of several different SRRs, rotated and/or re-dimensioned, in a unit cell. Analysis and design of this structure is provided through full-wave simulation model. Results for the three different SRRs in a unit cell are obtained. Results show increased bandwidth about 70% for the proposed structure. Moreover, we show that the SRR arrangement in the unit cell is crucial and should be based on a descending and/or ascending resonant frequency order. The measurement results achieved via a strip-line technique fully confirm this idea.

REFERENCES

1. Veselago, V. G., "The electrodynamics of substances with simultaneously negative values of epsilon and mu," *Sov. Phys. Uspekhi*, Vol. 10, 509–514, 1968.
2. Pendry, J. B., A. J. Holden, D. J. Robbins, and W. J. Stewart, "Magnetism from conductors and enhanced nonlinear phenomena," *IEEE Trans. Microw. Theory Tech.*, Vol. 47, No. 11, 2075–2084, Nov. 1999.
3. Shelby, R. A., D. R. Smith, and S. Schultz, "Experimental verification of a negative index of refraction," *Science*, Vol. 292, No. 6, 77–79, Apr. 2001.
4. Pendry, J. B., A. J. Holden, W. J. Stewart, and I. Youngs, "Extremely low frequency plasmons in metallic microstructures," *Phys. Rev. Lett.*, Vol. 76, No. 25, 4773–4776, 1996.
5. Chen, H., L. Ran, J. Huangfu, X. Zhang, K. Chen, T. M. Grzegorzcyk, and J. A. Kong, "Left-handed materials composed of only S-shaped resonators," *Phys. Rev. E*, Vol. 70, No. 5, 057605.1–057605.4, 2004.
6. Wu, B. I., W. Wang, J. Pacheco, X. Chen, T. Grzegorzcyk, and J. A. Kong, "Experimental confirmation of negative refractive index of a metamaterial composed of Ω -like metallic patterns," *App. Phys. Lett.*, Vol. 84, No. 9, 1537–1539, Mar. 2004.
7. Baena, J. D., R. Marques, F. Medina, and J. Martel, "Artificial magnetic metamaterial design by using spiral resonators," *Phys. Rev. B*, Vol. 69, No. 1, 014402.1–014402.5, 2004.
8. Ahmed, A. and M. A. Alsunaidi, "Design of wide-band

- metamaterials based on the split ring resonator,” *NATO ARW & META*, 523–528, 2008.
9. Sabah, C. and H. G. Roskos, “Broadband terahertz metamaterial for negative refraction,” *PIERS Proceedings*, 785–788, Moscow, Russia, Aug. 18–21, 2009.
 10. De La Mata Luque, T. M., N. R. Devarapalli, and C. G. Christodoulou, “Investigation of bandwidth enhancement in volumetric left-handed metamaterials using fractal,” *Progress In Electromagnetics Research*, Vol. 131, 185–194, 2012.
 11. Chowdhury, D. R., R. Singh, M. Reiten, H. Chen, A. J. Taylor, J. F. O’Hara, and A. K. Azad, “A broadband planar terahertz metamaterial with nested structure,” *Opt. Exp.*, Vol. 19, No. 17, 15817–15823, Aug. 2011.
 12. Huang, L., D. R. Chowdhury, S. Ramani, M. T. Reiten, S. N. Luo, A. J. Taylor, and H. T. Chen, “Experimental demonstration of terahertz metamaterial absorbers with a broad and flat high absorption band,” *Opt. Lett.*, Vol. 37, No. 2, 154–156, 2012.
 13. Rudolph, S. M. and A. Grbic, “Super-resolution focusing using volumetric, broadband NRI media,” *IEEE Trans. on Ant. and Pro.*, Vol. 56, No. 9, 2963–2969, Sep. 2008.
 14. Lepetit, T., E. Akmansoy, M. Pate, and J. P. Ganne, “Broadband negative magnetism from all-dielectric metamaterial,” *Electron. Lett.*, Vol. 44, No. 19, Sep. 2008.
 15. Cui, T. J., D. R. Smith, and R. Liu, *Metamaterials Theory, Design and Applications*, Springer, 2009.
 16. Wang, J., S. Qu, Z. Xu, H. Ma, Y. Yang, and C. Gu, “A controllable magnetic metamaterial: Split-ring resonator with rotated inner ring,” *IEEE Trans. on Ant. and Pro.*, Vol. 56, No. 7, 2018–2022, Jul. 2008.
 17. Cameron, R. J., R. Mansour, and C. M. Kudsia, *Microwave Filters for Communication Systems: Fundamentals, Design and Applications*, John Wiley and Sons, 2007.
 18. Chen, X., T. M. Grzegorzcyk, B. Wu, J. Pacheco, and J. A. Kong, “Robust method to retrieve the constitutive effective parameters of metamaterials,” *Phys. Rev. E*, Vol. 70, No. 1, 016608.1–016608.7, Jul. 2004.
 19. Yousefi, L., M. S. Boybay, and O. M. Ramahi, “Characterization of metamaterials using a strip line fixture,” *IEEE Trans. on Ant. and Pro.*, Vol. 59, No. 4, 1245–1253, Apr. 2011.